

Boosted $hh \rightarrow b\bar{b}b\bar{b}$: a new topology in searches for TeV-scale resonances at the LHC

Ben Cooper, Nikos Konstantinidis, Luke Lambourne, and David Wardrope
*Department of Physics and Astronomy, University College London,
Gower Street, London WC1E 6BT, United Kingdom*

It is widely believed that fully hadronic final states are not competitive in searches for new physics at the Large Hadron Collider due to the overwhelming QCD backgrounds. In this letter, we present a particle-level study of the topology arising when a TeV-scale resonance decays to two Higgs bosons and these subsequently decay to $b\bar{b}$, leading to two back-to-back boosted dijet systems. We show that selecting events with this topology dramatically reduces all backgrounds, thus enabling very competitive searches for new physics in a variety of models. For a resonance with mass 1 TeV and width around 60 GeV, we find that ATLAS or CMS could have a sensitivity to a $\sigma \times BR$ as small as a few fb with the LHC data collected in 2012. These conclusions are also relevant to the boosted $Zh \rightarrow b\bar{b}b\bar{b}$ and $ZZ \rightarrow b\bar{b}b\bar{b}$ final states, which would further increase the potential sensitivity to new physics as well as to Standard Model processes like longitudinal vector boson scattering.

Since the start of collision data-taking in 2009, the LHC experiments have performed numerous analyses searching for high mass resonances at the TeV scale. With few exceptions [1–4], such searches have relied on final states containing leptons (electrons or muons), for example: $Z' \rightarrow \ell^+\ell^-$ [5, 6]; resonant diboson production (WW , WZ , ZZ) [7–9], where at least one vector boson decays to leptons; or searches for resonances decaying to $t\bar{t}$ [10–12], where one or both of the top quarks decay semi-leptonically. The main reasons for this choice are that the presence of leptons helps to drastically reduce the QCD backgrounds, and that such final states are relatively easy to trigger on in ATLAS and CMS. However, the low branching ratios of the leptonic decays of the vector bosons, particularly of the Z , mean that the above searches are not sensitive to a large fraction of the production cross section of possible new resonances. In addition, resonances with masses at the TeV scale generally have a large natural width (typically tens of GeV or more), so the good experimental mass resolution offered by the leptonic channels does not improve the search sensitivity as much as for low mass resonances, where strict mass selection criteria are possible due to small widths. Finally, in many theoretical models [13–15], high mass resonances often decay with a sizeable branching ratio to a pair of Higgs bosons and since the Standard Model (SM) predicts the dominant decay of the Higgs to be to $b\bar{b}$, trying to look for final states involving leptons (or photons) from the Higgs decays leads to a significant effective reduction of the signal cross section.

Motivated by these arguments and by the discovery of the Higgs boson [16, 17], h , which appears to be consistent with the SM expectations, we have performed a particle-level analysis to evaluate the LHC sensitivity to TeV-scale resonances decaying to hh and subsequently to $b\bar{b}b\bar{b}$. For resonances of this mass scale, the two Higgs bosons will have high transverse momenta, resulting in two highly boosted, back-to-back $b\bar{b}$ dijet systems. This topology has several advantages: (i) requiring four b -tagged jets paired into two boosted dijets is a very pow-

erful way to drastically reduce backgrounds, in particular QCD; (ii) there is negligible ambiguity in pairing the four b -jets to correctly reconstruct the Higgs decays; and (iii) due to the high boost, the four jets will have high enough transverse momenta for such events to be selected with high efficiency at the first level trigger of ATLAS and CMS, with efficient High Level triggering possible through online b -tagging. The same topology will also arise for any high mass resonance decaying to $b\bar{b}b\bar{b}$ via Zh or ZZ . In the following, we focus on the $hh \rightarrow b\bar{b}b\bar{b}$ final state, but the conclusions of this study are also relevant for the $Zh \rightarrow b\bar{b}b\bar{b}$ and $ZZ \rightarrow b\bar{b}b\bar{b}$ final states.

The signal used as a benchmark in this study is a Randall-Sundrum [13] Kaluza-Klein (KK) graviton, G_{KK} , decaying to hh , but several other models beyond the SM lead to this topology, for example $H \rightarrow hh$ in two-Higgs-doublet models (2HDM) [14], or in singlet extensions to the SM Higgs sector [15]. Furthermore, this topology will also arise in: (i) decays of the pseudoscalar Higgs boson of 2HDM, $A \rightarrow Zh$; and (ii) longitudinal ZZ boson scattering at the TeV scale. The latter offers an alternative channel with which to measure the vector boson scattering cross section and to search for possible resonances that may modify this.

The KK graviton signal is generated using MadGraph [20] based on the scenario proposed in [18, 19] with $k/\bar{M}_{\text{Pl}} = 1$. The CTEQ6L1 parton density functions (PDFs) [21] were used and MadGraph was interfaced to Pythia 8.170 [22] for parton showering, hadronization and underlying event simulation. Table I shows the width and predicted production cross section for various graviton masses, m_G .

The event selection starts by requiring at least four b -tagged jets with $p_T > 40$ GeV and $|\eta| < 2.5$. Jets are formed using the anti- k_T algorithm [23] with radius parameter $R = 0.4$, implemented in Fastjet [24]. In order to estimate the effect of b -tagging, jets are labeled as b -jets, c -jets or light jets depending on the flavor of partons within $\Delta R < 0.3$ of the jet axis. If a b -quark is found, the

Graviton Mass [GeV]	$\sigma(pp \rightarrow G_{KK} \rightarrow hh \rightarrow b\bar{b}b\bar{b})$ [fb]	Γ [GeV]
500	329	18.6
700	72.7	33.9
900	18.6	48.6
1100	5.51	62.7
1300	1.82	76.5
1500	0.65	90.0

TABLE I. Mass, cross section and width of the KK graviton signal.

jet is labeled a b -jet, otherwise if a c -quark is found the jet is labeled a c -jet. If neither a b -quark nor a c -quark is found, then the jet is classified as a light jet. We then apply b -tagging efficiency factors, based on the published ATLAS and CMS b -tagging performance [25, 26]: 70% for b -labeled jets, 20% for c -labeled jets (“rejection factor” 5) and 1% for light-labeled jets (“rejection factor” 100). Dijets are then formed, requiring $p_T^{\text{dijet}} > 200$ GeV and $\Delta R_{\text{dijet}} = \sqrt{\Delta\phi^2 + \Delta\eta^2} < 1.2$, where $\Delta\phi$ is the angular separation between jets in the plane transverse to the beam line and $\Delta\eta$ is the difference in pseudorapidity between the two jets. Finally, we require a dijet invariant mass, m_{dijet} , consistent with h decay. In the extremely rare cases where more than two dijets satisfy all the above requirements, only the two dijets with the highest p_T^{dijet} are considered.

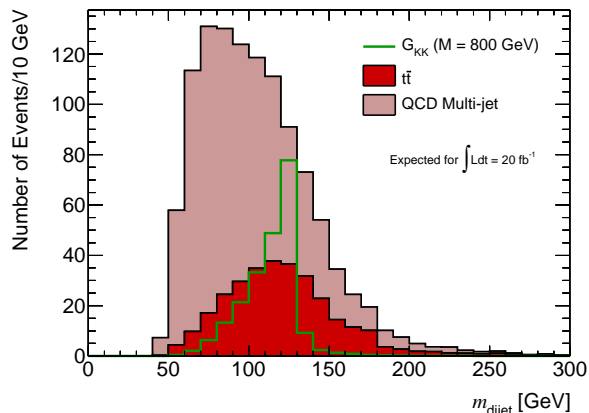


FIG. 1. The individual dijet mass distributions in signal and background (stacked).

The dijet mass distributions in the signal and background are shown in Fig. 1 for $m_h = 125$ GeV. It can be seen that the Higgs mass peak in the signal is shifted to lower masses. This is because, in this particle-level study, the reconstructed jets do not include neutrinos and muons or any out-of-cone corrections. Hence, we have chosen the Higgs mass window to be $100 < m_{\text{dijet}} <$

130 GeV. This study has not considered detector resolution effects that will smear the jet p_T measurements and broaden the four-jet invariant mass, m_{4b} . However, for resonances with natural width some tens of GeV or more, the detector resolution is not expected to increase the width of the observed peak significantly. Moreover, it is possible to take advantage of the known mass of the two Higgs bosons and perform a kinematic fit to determine m_{4b} , which will largely remove the detector resolution effects. The impact of additional pile-up interactions has also not been considered in this study, since for jets with $p_T > 40$ GeV and $|\eta| < 2.5$ both ATLAS and CMS have demonstrated that pile-up effects can be strongly mitigated [27, 28].

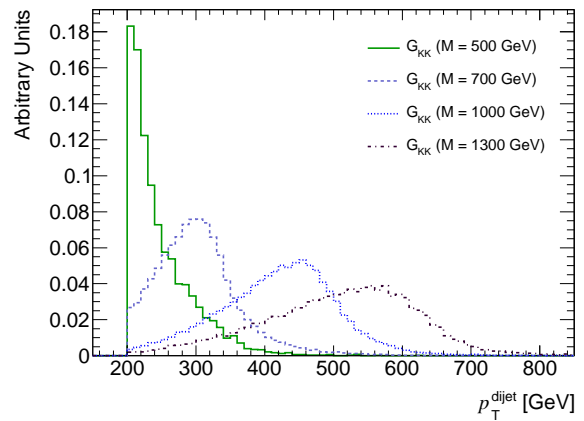


FIG. 2. The p_T^{dijet} distribution for different graviton masses.

The p_T^{dijet} distribution is shown in Fig. 2 for various signal masses. It can be seen that for $m_G = 500$ GeV, the $p_T^{\text{dijet}} > 200$ GeV requirement has a visible impact on the signal acceptance and would need to be optimized to achieve the best possible sensitivity to masses around 700 GeV and below. Similarly, for higher signal masses, the optimal p_T^{dijet} requirement would likely be higher than 200 GeV.

The ΔR_{dijet} distribution in the dijet systems is shown in Fig. 3 for various signal masses. It can be seen that for high graviton masses the two b -jets from the h decay tend to get closer and closer, hence with increasing likelihood merge into a single jet, leading to selection inefficiencies. This inefficiency can be dealt with in a number of ways: (i) by forming narrower jets in the search for higher mass signals; (ii) by identifying two separate b -hadron decay vertices within single, energetic jets, as in [29]; or (iii) by using jet substructure techniques [30, 31] and applying b -tagging to the individual sub-jets. These alternatives should be explored in order to extend the sensitivity of this search to as high a resonance mass as possible. At the other end of the mass spectrum, the requirement $\Delta R_{\text{dijet}} < 1.2$ may be an impediment for $m_G < 700$ GeV

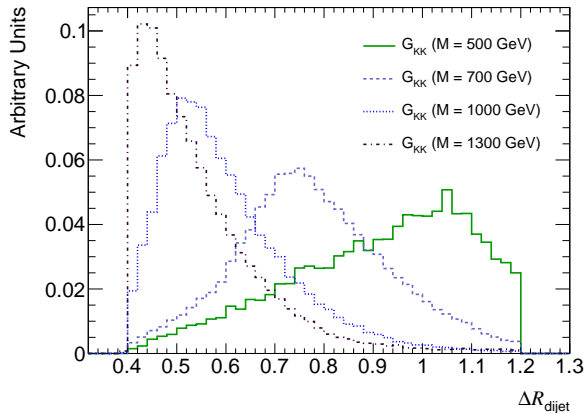


FIG. 3. The ΔR_{dijet} distribution for different graviton masses.

and should be revisited for extending the sensitivity of the search to lower resonance masses.

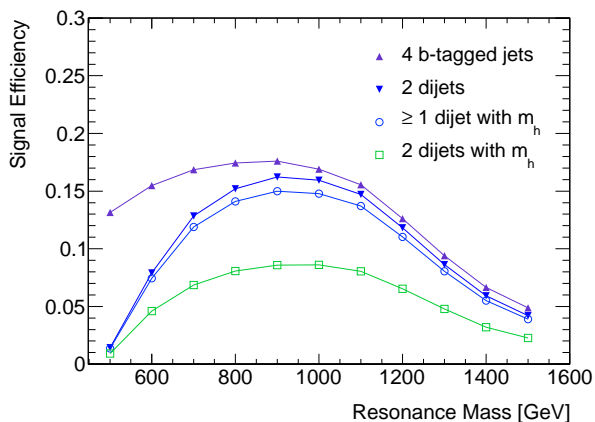


FIG. 4. The evolution of signal efficiency at each step of the analysis.

The signal efficiency through the cut flow of the above selection is shown in Fig. 4. This confirms the observations made above about signal efficiency losses at the low and high ends of the resonance mass range considered in this study. The biggest efficiency drop comes from the b -tagging requirement, approximately ($0.7^4 \approx 0.24$).

The backgrounds to this search are the irreducible $pp \rightarrow b\bar{b}b\bar{b}$ and those reducible backgrounds resulting from the false classification of jets as b -jets, such as $t\bar{t}$ or $pp \rightarrow b\bar{b}c\bar{c}$. Other backgrounds, such as diboson production or Z +jets events, were found to be negligible due to the requirement that the dijet masses fall within the h mass range.

The $pp \rightarrow b\bar{b}b\bar{b}$ and other QCD multi-jet backgrounds have been simulated using Sherpa 1.4.3 [32], with which we generate events based on tree-level matrix elements

with four partons in the final state. After b -tagging, the QCD multi-jet background is dominated by $pp \rightarrow b\bar{b}b\bar{b}$, with a smaller contribution from mistagged $pp \rightarrow b\bar{b}c\bar{c}$ events. The accuracy of the simulation of $pp \rightarrow b\bar{b}b\bar{b}$ by Sherpa is verified by reproducing a total cross-section approximately equal to the leading order prediction from [33] and [34]. The uncertainty due to missing higher order matrix element terms in $pp \rightarrow b\bar{b}b\bar{b}$ and $pp \rightarrow b\bar{b}c\bar{c}$ is estimated by varying the renormalization and factorization scales by factors of 1/2 and 2 from their nominal values of $\frac{1}{4} \sqrt{\sum_i p_{T,i}^2}$. It was found in [33] that this variation covers the NLO prediction. Consequently, we are confident that our estimate of this background is reliable within its uncertainty.

The $t\bar{t}$ background was simulated using Pythia 8.170, with the cross section scaled to the average cross section measured by ATLAS and CMS at 8 TeV [35, 36]. We find that the flavor composition of the four-jet system in the $t\bar{t}$ events passing the full selection is predominantly $bc - bc$, which occurs when both t -quarks decay hadronically, as $t \rightarrow bW \rightarrow bcs$, and the b and c jets end up nearby. The uncertainty on the measured cross section is propagated as the uncertainty on the $t\bar{t}$ background estimate.

Requirement	$G_{\text{KK}}(M = 800 \text{ GeV})$	QCD	$t\bar{t}$
4 b -tagged jets	126	19700	3590
2 dijets	109	414	151
≥ 1 dijet with m_h	102	183	89
2 dijets with m_h	58	28^{+20}_{-11}	21 ± 3

TABLE II. Event selection, showing the expected signal and background yields for $\int \mathcal{L} dt = 20 \text{ fb}^{-1}$ at $\sqrt{s} = 8 \text{ TeV}$.

Table II shows the expected yields for a graviton signal with mass 800 GeV and the QCD and $t\bar{t}$ backgrounds, along with their uncertainties. Thanks to the powerful background rejection from the event topology requirements, the signal to background ratio is approximately 1 for this benchmark model, demonstrating the sensitivity of this analysis to signals with very low cross section.

The m_{4b} distribution for signal and background is shown in Fig. 5. To estimate the boosted $b\bar{b}b\bar{b}$ search sensitivity for 20 fb^{-1} of pp collisions at $\sqrt{s} = 8 \text{ TeV}$, as a function of the mass of a graviton-like resonance, we define mass windows around the resonance mass, m_X , as $[m_X - 100, m_X + 50]$ (in GeV). We then determine the signal efficiency and expected number of background events, N_{bkg} , within these windows, and calculate the cross section $\sigma(pp \rightarrow X \rightarrow hh \rightarrow b\bar{b}b\bar{b})$ that would give $3 \times \sqrt{N_{bkg}}$ signal events. These estimates of the 3σ observation sensitivity are shown in Fig. 6. It can be seen that around 1 TeV the analysis achieves the best sensitivity, to cross-sections down to a few fb. At lower and higher masses the loss of signal acceptance mentioned above de-

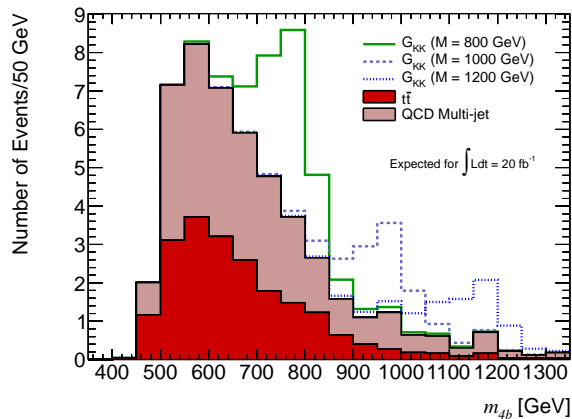


FIG. 5. The stacked m_{4b} distribution for various signal masses and for the background. The signal production cross-sections are normalized to those required for 3σ evidence in 20 fb^{-1} of pp collisions at $\sqrt{s} = 8 \text{ TeV}$.

creases the sensitivity, but as already commented, there is scope for optimization that could bring the sensitivity to $O(10\text{fb})$ in these regions, and extend the reach much beyond the mass range considered here. Although experimental systematics that would worsen the sensitivity have not been considered, large gains in sensitivity are possible through an overall optimization of the analysis. These results should apply equally well to any model that predicts a high mass resonance decaying to hh , provided that its natural width is similar to that of the KK graviton used in this study. For the KK graviton model used here, Fig. 6 shows that this analysis would give more than 3σ sensitivity up to the TeV scale.

For many new physics models [14, 15], where the decay of the intermediate resonance to anything other than hh can be strongly suppressed, the results in Fig. 6 represent a unique sensitivity. For others, the sensitivities shown in Fig. 6 could be surpassed by combining the $hh \rightarrow b\bar{b}b\bar{b}$ search with other channels and final states. For example, in the signal model used in this letter the KK graviton decays to both hh and ZZ with branching fractions around 10%. A KK graviton search in the $b\bar{b}b\bar{b}$ final state combining both ZZ and hh channels would increase considerably the sensitivity to such a signal, and could be further combined with the already explored WW and ZZ search channels that don't involve b -quarks in the final state [3, 7–9].

We conclude that the final state topology of two, boosted, b -tagged dijet systems shows great promise for increasing the LHC sensitivity to TeV-scale resonances decaying into a pair of electroweak-scale bosons, such as hh , Zh or ZZ . It combines low background levels with good acceptance to various signal processes, making it a powerful channel in which to search for new physics, both in the current LHC data and in the higher energy

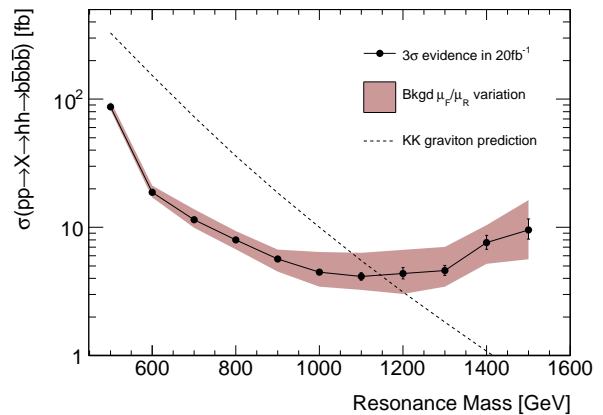


FIG. 6. The signal cross section required in 20 fb^{-1} of pp collisions at $\sqrt{s} = 8 \text{ TeV}$ for achieving a 3σ evidence of $pp \rightarrow X \rightarrow hh \rightarrow b\bar{b}b\bar{b}$. The error bars indicate the statistical uncertainties, and the shaded band the QCD background renormalization and factorization scale uncertainties. The $G_{KK} \rightarrow hh \rightarrow b\bar{b}b\bar{b}$ cross section from Table I is displayed as the dashed curve.

running from 2015 onwards.

-
- [1] CMS Collaboration, JHEP **1301** (2013) 013.
 - [2] CMS Collaboration, arXiv:1302.4794 [hep-ex].
 - [3] CMS Collaboration, Phys.Lett. **B723** (2013) 280–301.
 - [4] ATLAS Collaboration, Tech. Rep. ATLAS-CONF-2012-148, CERN, Geneva, 2012.
 - [5] ATLAS Collaboration, JHEP **1211** (2012) 138.
 - [6] CMS Collaboration, Phys.Lett. **B720** (2013) 63–82.
 - [7] CMS Collaboration, JHEP **1302** (2013) 036.
 - [8] ATLAS Collaboration, Phys. Rev. D **87** (2013) 112006.
 - [9] ATLAS Collaboration, Tech. Rep. ATLAS-CONF-2012-150, CERN, Geneva, 2012.
 - [10] CMS Collaboration, Phys.Rev. **D87** (2013) 072002.
 - [11] ATLAS Collaboration, arXiv:1305.2756 [hep-ex].
 - [12] ATLAS Collaboration, Tech. Rep. ATLAS-CONF-2013-052, CERN, Geneva, 2013.
 - [13] L. Randall and R. Sundrum, Phys.Rev.Lett. **83** (1999) 3370–3373.
 - [14] B. Coleppa, F. Kling, and S. Su, arXiv:1305.0002 [hep-ph].
 - [15] G. M. Pruna and T. Robens, arXiv:1303.1150 [hep-ph].
 - [16] ATLAS Collaboration, Phys.Lett. **B716** (2012) 1–29.
 - [17] CMS Collaboration, Phys.Lett. **B716** (2012) 30–61.
 - [18] K. Agashe, H. Davoudiasl, G. Perez, and A. Soni, Phys. Rev. **D76** (2007) 036006.
 - [19] L. Fitzpatrick, J. Kaplan, L. Randall, and L.-T. Wang, JHEP **2007** (2007) 013.
 - [20] J. Alwall, M. Herquet, F. Maltoni, O. Mattelaer, and T. Stelzer, JHEP **1106** (2011) 128.
 - [21] D. Stump, J. Huston, J. Pumplin, W.-K. Tung, H. Lai, et al., JHEP **0310** (2003) 046.
 - [22] T. Sjostrand, S. Mrenna, and P. Z. Skands,

- Comp.Phys.Com. **178** (2008) 852–867.
- [23] M. Cacciari, G. P. Salam, and G. Soyez, JHEP **0804** (2008) 063.
- [24] M. Cacciari, G. P. Salam and G. Soyez, Eur. Phys. J. C **72** (2012) 1896.
- [25] CMS Collaboration, JINST **8** (2013) P04013.
- [26] ATLAS Collaboration, Tech. Rep. ATLAS-CONF-2012-097, CERN, Geneva, 2012.
- [27] ATLAS Collaboration, Tech. Rep. ATLAS-CONF-2013-083, CERN, Geneva, 2013.
- [28] CMS Collaboration, Tech. Rep. CMS-PAS-JME-13-005, CERN, Geneva, 2013.
- [29] ATLAS Collaboration, EPJ **C73** (2013) no. 2, 1–30.
- [30] J. M. Butterworth, A. R. Davison, M. Rubin, and G. P. Salam, Phys.Rev.Lett. **100** (2008) 242001.
- [31] M. Gouzevitch, A. Oliveira, J. Rojo, R. Rosenfeld, G. P. Salam and V. Sanz, JHEP **1307**, 148 (2013).
- [32] T. Gleisberg, S. Hoeche, F. Krauss, M. Schonherr, S. Schumann, et al. JHEP **0902** (2009) 007.
- [33] N. Greiner, A. Guffanti, T. Reiter, and J. Reuter, Phys. Rev. Lett. **107** (Sep, 2011) 102002.
- [34] G. Bevilacqua, M. Czakon, M. Krämer, M. Kubocz, and M. Worek, [arXiv:1304.6860](https://arxiv.org/abs/1304.6860) [hep-ph].
- [35] ATLAS Collaboration, Tech. Rep. ATLAS-CONF-2012-149, CERN, Geneva, 2012.
- [36] CMS Collaboration, Tech. Rep. CMS-PAS-TOP-12-027, CERN, Geneva, 2013.